

1 **Ice core chemistry database: an Antarctic compilation of**  
2 **sodium and sulphate records spanning the past 2000 years.**

3 Elizabeth R. Thomas<sup>1</sup>, Diana O. Vladimirova<sup>1</sup>, Dieter Tetzner<sup>1</sup>, B. Daniel Emanuelsson<sup>1</sup>,  
4 Nathan Chellman<sup>2</sup>, Daniel A. Dixon<sup>3</sup>, Hugues Goosse<sup>4</sup>, Mackenzie M. Grieman<sup>5</sup>, Amy C.F.  
5 King<sup>1</sup>, Michael Sigl<sup>6</sup>, Danielle G Udy<sup>7</sup>, Tessa R. Vance<sup>8</sup>, Dominic A. Winski<sup>3</sup>, V. Holly L.  
6 Winton<sup>9</sup>, Nancy A.N. Bertler<sup>9,10</sup>, Akira Hori<sup>11</sup>, Chavarukonam.M Laluraj<sup>12</sup>, Joseph R.  
7 McConnell<sup>2</sup>, Yuko Motizuki<sup>13</sup>, Kazuya Takahashi<sup>13</sup>, Hideaki Motoyama<sup>14</sup>, Yoichi Nakai<sup>13</sup>,  
8 Franciele Schwanck<sup>15</sup>, Jefferson Cardia Simões<sup>15</sup>, Filipe G. L. Lindau<sup>15</sup>, Mirko Severi<sup>16</sup>, Rita  
9 Traversi<sup>16</sup>, Sarah Wauthy<sup>17</sup>, Cunde Xiao<sup>18</sup>, Jiao Yang<sup>19</sup>, Ellen Mosely-Thompson<sup>20</sup>, Tamara  
10 V. Khodzher<sup>21</sup>, Ludmila P. Golobokova<sup>21</sup>, Alexey A. Ekaykin<sup>22</sup>

11  
12 <sup>1</sup>Ice Dynamics and Paleoclimate, British Antarctic Survey, High Cross, Madingley Road, Cambridge,  
13 CB3 0ET, UK

14 <sup>2</sup>Division of Hydrologic Sciences, Desert Research Institute, Reno, NV, 89512, USA

15 <sup>3</sup>Climate Change Institute, University of Maine, 5790 Bryand Global Science Center, Orono, ME,  
16 04469, USA.

17 <sup>4</sup>Earth and Life Institute, Universite catholique de Louvain, Place Pasteur 3, 1348 Louvain-la-Neuve,  
18 Belgium

19 <sup>5</sup>Department of Chemistry, Reed College, 3203 Woodstock Blvd., Portland, Oregon, 97202, USA

20 <sup>6</sup>Climate and Environmental Physics (CEP), Physics Institute & Oeschger Centre for Climate Change  
21 Research (OCCR), University of Bern, Sidlerstrasse 5, 3012 Bern, Switzerland

22 <sup>7</sup>Institute for Marine and Antarctic Studies, University of Tasmania, 20 Castray Esplanade, Battery  
23 Point TAS 7004, Australia

24 <sup>8</sup>Australian Antarctic Program Partnership, Institute for Marine & Antarctic Studies, University of  
25 Tasmania, Hobart, Australia

26 <sup>9</sup>Antarctic Research Centre, Victoria University of Wellington, Kelburn Parade, Kelburn, Wellington  
27 6021, New Zealand

28 <sup>10</sup>National Ice Core Facility, GNS Science, 30 Gracefield Rd, Gracefield 5040, New Zealand

29 <sup>11</sup>Kitami Institute of Technology, 090-8507, Japan

30 <sup>12</sup>National Centre for Polar and Ocean Research (NCPOR), Ministry of Earth Sciences, Vasco-da  
31 Gama, Goa 403804, India

32 <sup>13</sup>RIKEN Nishina Center for Accelerator-Based Science, 2-1 Hirosawa, Wako, Saitama 351-0198,  
33 Japan

34 <sup>14</sup>National Institute of Polar Research, Tachikawa, Tokyo 190-8518, Japan

35 <sup>15</sup>Centro Polar e Climático, Universidade Federal do Rio Grande do Sul, Porto Alegre, 91501-970,  
36 Brazil

37 <sup>16</sup>Chemistry Dept. "Ugo Schiff", University of Florence, 50019, Sesto F.no, Florence, Italy.

38 <sup>17</sup>Laboratoire de Glaciologie, Department Geosciences, Environnement et Societe, Universite Libre de  
39 Bruxelles, 1050 Brussels, Belgium

40 <sup>18</sup>State Key Laboratory of Earth Surface Processes and Resource Ecology, Beijing Normal University,  
41 China

42 <sup>19</sup>State Key Laboratory of Cryospheric Science, Northwest Institute of Eco-Environment and  
43 Resources, Chinese Academy of Sciences, Lanzhou 730000, China

44 <sup>20</sup>Byrd Polar and Climate Research Center, The Ohio State University, 1090 Carmack Rd. Columbus  
45 OH 43210 USA

46 <sup>21</sup>Limnological Institute of Siberian Branch of the Russian Academy of Sciences), Irkutsk, 664033,  
47 Russia

48 <sup>22</sup> Arctic and Antarctic Research Institute), 38 Bering st, St Petersburg, 199397, Russia

49 *Correspondence to:* Elizabeth R. Thomas ([lith@bas.ac.uk](mailto:lith@bas.ac.uk))  
50

51

52

53

54

55

56

57

58

59

60

61

62

63

64

65

66

67

68

69

70

71

72

73

74 **Abstract.** Changes in sea ice conditions and atmospheric circulation over the Southern Ocean play an important  
75 role in modulating Antarctic climate. However, observations of both sea ice and wind conditions are limited in  
76 Antarctica and the Southern Ocean, both temporally and spatially, prior to the satellite era (1970 onwards). Ice  
77 core chemistry data can be used to reconstruct changes over annual, decadal, and millennial timescales. To  
78 facilitate sea ice and wind reconstructions, the CLIVASH2k working group has compiled a database of two  
79 species, sodium [Na<sup>+</sup>] and sulphate [SO<sub>4</sub><sup>2-</sup>], commonly measured ionic species. The database ~~contains~~ **comprises**  
80 records from 105 Antarctic ice cores, containing records with a maximum age duration of 2000 years. An initial  
81 filter has been applied, based on evaluation against [sea ice concentration, geopotential heights \(500 hPa\) and](#)  
82 [surface wind fields](#) ~~climate observations~~, to identify sites suitable for reconstructing past sea ice conditions,  
83 wind strength, or atmospheric circulation.

84

85

## 86 1 Introduction

87 Changes in wind strength and atmospheric circulation, notably the positive phase of the Southern Annular Mode  
88 (SAM), have been related to increased Antarctic snowfall (Thomas et al., 2017; Thomas et al., 2008; Medley  
89 and Thomas, 2019) and the widespread warming in the Antarctic Peninsula (Turner et al., 2016; Thomas et al.,  
90 2009) and West Antarctica during the 20th century. Contemporaneously, Antarctic sea ice is also undergoing  
91 significant change. Despite model predictions of a homogeneous decline (Roach et al., 2020), total Antarctic sea  
92 ice cover has increased since 1970 (Zwally et al., 2002; Turner et al., 2009). With more recent periods of abrupt  
93 decline in 2016, (Meehl et al., 2016) and 2022 (Turner et al., 2022).

94 Our understanding of winds, atmospheric circulation and sea ice is hampered by both the lack of observations  
95 prior to the instrumental period (~1970s onwards) and uneven spatial coverage of paleoclimate records (Jones et  
96 al., 2016; Thomas et al., 2019). Data-model intercomparison and data synthesis studies have demonstrated the  
97 value of large datasets in reconstructing climate and sea ice **variability** over decadal to centennial **time** scales  
98 (Dalaiden et al., 2021; Fogt et al., 2022). To meet the need for Antarctic-wide, spatially dense, and  
99 intercomparable atmospheric circulation and sea ice records, we propose the use of chemical species routinely  
100 measured in ice cores.

101 Sodium [Na<sup>+</sup>], from sea salt aerosol, has been proposed as a proxy for past sea ice extent (SIE)  
102 ([Waisdivideprojectmembers et al., 2013](#); Severi et al., 2017; Wolff et al., 2006; Winski et al., 2021;  
103 [Wais\\_Divide\\_Project\\_Members., 2013](#)). The sea salt component of [Na<sup>+</sup>] arises from both sea ice and open  
104 water and the relationship between [Na<sup>+</sup>] and sea ice varies between sites (Sneed et al., 2011). High winds  
105 mobilize [Na<sup>+</sup>] from the sea ice surface, either in frost flowers or brine-soaked snow (Huang and Jaeglé, 2017;  
106 Frey et al., 2020). The [Na<sup>+</sup>] reaching the ice core sites is dependent on both the distances from the source,  
107 either sea ice or open ocean, and the meteorological conditions (Minikin et al., 1994; Rhodes et al., 2018). [Na<sup>+</sup>]  
108 is therefore a valuable tracer for marine-air mass advection and changes in atmospheric circulation (Dixon et al.,  
109 2004; Mayewski et al., 2017).

110 Sulphate [SO<sub>4</sub><sup>2-</sup>] is formed in the atmosphere as secondary aerosol following volcanic and anthropogenic  
111 sulphur dioxide [SO<sub>2</sub>] gas emissions. [SO<sub>4</sub><sup>2-</sup>], together with methane sulphonic acid [MSA], is the main  
112 atmospheric sulphur compound formed from ocean-derived dimethylsulfide (DMS) (Gondwe et al., 2003). In  
113 the southern hemisphere, marine biogenic emissions dominate the total sulphur budget (Delmas et al., 1982;  
114 Legrand and Mayewski, 1997; Mccoy et al., 2015). Sulphur can significantly impact cloud albedo and new  
115 particle formation (Brean et al., 2021). The sea salt fraction of [SO<sub>4</sub><sup>2-</sup>] is largest at coastal and low elevation sites  
116 (Dixon et al., 2004). The non-sea salt fraction, also referred to as excess [SO<sub>4</sub><sup>2-</sup>] (hereafter referred to as xs  
117 [SO<sub>4</sub><sup>2-</sup>]), can be estimated based on the relationship with [Na<sup>+</sup>] (e.g.,  $xs [SO_4^{2-}] = [SO_4^{2-}] - 0.25[Na^+]$ ) (O'Brien et  
118 al., 1995). Excess [SO<sub>4</sub><sup>2-</sup>] has been shown to correlate with SIE at some ice core sites (Dixon et al., 2004; Sneed  
119 et al., 2011). The background xs [SO<sub>4</sub><sup>2-</sup>] source, from marine biogenic deposition, is superimposed by sporadic  
120 volcanic deposition of [SO<sub>4</sub><sup>2-</sup>] providing an excellent reference horizon for dating Antarctic ice cores (Dixon et  
121 al., 2004; Sigl et al., 2014; Plummer et al., 2012). At low elevation and coastal sites, where background biogenic  
122 sources are high, it is not always possible to identify volcanic peaks (Emanuelsson et al., 2022; Tetzner et al.,  
123 2021b). In this study, [SO<sub>4</sub><sup>2-</sup>] provides a dual function: 1) as a potential proxy for SIE and 2) as a stratigraphic

124 age marker to validate submitted age-scales and subsequently align ice-core chronologies onto a common  
125 chronology.

### 126 1.1. The CLIVASH2k chemistry database.

127 CLIVASH2k (CLimate Variability in Antarctica and the Southern Hemisphere over the past 2000 years) is a  
128 project of the Past Global Changes (PAGES) 2k network. The CLIVASH2k database is the latest in a series of  
129 community-led paleoclimate data synthesis efforts endorsed by PAGES (Kaufman et al., 2020; Mcgregor et al.,  
130 2015; McKay and Kaufman, 2014; Tierney et al., 2015; Thomas et al., 2017; Stenni et al., 2017; Konecky et al.,  
131 2020). The aim of this study is to focus on two primary species, sodium, and sulphate, as they are routinely  
132 measured in ice cores and have potential links with either sea ice or atmospheric circulation. The time window  
133 of the last 2000 years has been selected to cover both natural and anthropogenic changes.

134 Two main features distinguish the CLIVASH2k data compilation from previous PAGES synthesis: 1) the data  
135 included are not limited to previously published records, and 2) the data comprise two distinct chemical species  
136 which do not have a well-established relationship with climate. ~~This differs from previous compilations where  
137 the data can be either directly, or indirectly, compared with a modelled or observed climate parameter e.g.  
138 temperature (Stenni et al., 2017), (beyond the episodic sources of [SO<sub>4</sub><sup>2-</sup>] noted above).~~

139 Calls for participation in CLIVASH2k activities were widely distributed, ensuring a ~~representative~~ cross section  
140 of scientists from various disciplines, geographic regions, and career stage. The targeted species to target and the  
141 selection criteria were decided at several open discussion stages, followed by updates to the CLIVASH2k  
142 mailing list and distributed via PAGES monthly updates.

## 143 2. Methods

144

### 145 2.1. Resolution and duration.

146 The target time-period for the database is the last 2000 years. Records of any duration could be submitted within  
147 this time-period. These records could be from snow-pits and firn cores, spanning just a few seasons to years.  
148 Data were requested at the highest resolution available and converted to annual averages (January – December).  
149 ~~Years with missing data were included, providing a threshold of half a year of data was achieved.~~

150

### 151 2.2. Age-scales.

152 Most records within this time-period have been annually dated, based on the seasonal deposition of distinct  
153 chemical species (including sodium, sulphate, and sulphur). The longer records, those spanning the last 500-  
154 2000 years, have been synchronized previously (Sigl et al., 2014) or within this project on the WD2014 age-  
155 scale (Sigl et al., 2016) or have age-scales that are broadly consistent with WD2014 (Plummer et al., 2012). This  
156 new chronology is constrained by the 774 CE cosmogenic (i.e. <sup>10</sup>Be) anomaly, and is consistent with  
157 dendrochronology (Büntgen et al., 2018) and ice core chronologies from Greenland (Sigl et al., 2015). The  
158 WD2014 age-scale is recommended because it is consistent with the forcings applied in PMIP4/CMIP6 model  
159 simulations (Jungclaus et al., 2017). Age transfer functions can now be linked to other PAGES2k  
160 reconstructions and individual ice cores. ~~There~~ ~~There~~ are ~~two a few~~ exceptions, Plateau Remote and DT401<sub>1</sub>  
161 (both very low accumulation sites in the interior of east Antarctica), ~~have been dated using [SO<sub>4</sub><sup>2-</sup>]~~ (Ren et al.,  
162 2010), ~~however, the reference which differ~~ horizons differ from WD2014 ~~age-scale~~ prior to 1000 AD and  
163 cannot be confidently synchronized. ~~The third~~ ~~Another~~ exception is partly unpublished data from the Vostok  
164 vicinity, which were dated using the snow accumulation rate and volcanic age markers (this study and (Ekaykin  
165 et al., 2014).

166

### 167 2.3. Peer review and publications.

168 Unlike previous PAGES 2k compilations, the CLIVASH2k database was not constrained by the need for  
169 records to be published and peer reviewed. This decision arose based on the limited number of published  
170 chemistry records available and the desire to maximise the records. Published records were submitted along  
171 with their original citation; unpublished records were listed as “This study”, with the data contributor included  
172 as a co-author.

173

174 **2.4. Analytical methods.**

175 Both the ionic and elemental forms of sodium ([Na] and [Na<sup>+</sup>]) and sulphur ([S] and [SO<sub>4</sub><sup>2-</sup>]), respectively, were  
176 accepted as part of the CLIVASH2k data call. Several analytical techniques are used to measure [Na<sup>+</sup>], [S] and  
177 [SO<sub>4</sub><sup>2-</sup>] in ice cores. Ionic [Na<sup>+</sup>] and [SO<sub>4</sub><sup>2-</sup>] are typically measured by ion chromatography (IC), while elemental  
178 Na and S are generally measured by inductively coupled plasma mass spectrometry (ICP-MS). Unlike IC, which  
179 measures the soluble fraction, ICP-MS techniques measure the total elemental concentration of both the  
180 dissolved and particulate fraction of the element. However, we note that there are different protocols for  
181 acidifying the samples prior to analysis which may result in different absolute concentrations, including the  
182 choice of acid, the acid concentration, and the acidification time. While continuous ICP-MS measurements of  
183 certain species may require correction for under-recovery, Na and S are typically fully recovered during  
184 continuous measurements (Arienzo et al., 2019). Previous comparisons of analytical methods show excellent  
185 agreement of [Na] in ice cores measured using IC and ICP-MS methods e.g. (Grieman et al., 2022). This  
186 agreement suggests that the ionic and elemental forms reported in the database can be directly compared.  
187

188 Biogenic atmospheric emissions of organic [S] species, mainly dimethyl sulfide (DMS), are a major contributor  
189 to the [S] in the Antarctic snow (Legrand and Mayewski, 1997). In the marine atmosphere DMS is oxidized to  
190 [MSA<sup>-</sup>] and [SO<sub>4</sub><sup>2-</sup>], which are eventually deposited on the polar ice sheets (Barnes et al., 2006). The ICP-MS  
191 technique measures total [S] in ice cores, which includes [S] contained [MSA<sup>-</sup>]. In contrast, the IC technique  
192 solely quantifies [S]. If total [S] and [MSA<sup>-</sup>] are both analysed on the same ice core, the [MSA<sup>-</sup>] contribution  
193 can be subtracted (Cole-Dai et al., 2021). However, continuous [MSA<sup>-</sup>] measurements are scarce over Antarctica  
194 (Thomas et al., 2019) and the long-term variability of both [MSA<sup>-</sup>] and [SO<sub>4</sub><sup>2-</sup>] is very small during the common  
195 era (Legrand et al., 1992; Saltzman et al., 2006). Thus, we applied a consistent transformation across all sites.  
196 We multiplied elemental [S] (32 g mol<sup>-1</sup>) from ICP-MS measurements with three to convert to the equivalent  
197 [SO<sub>4</sub><sup>2-</sup>] (96 g mol<sup>-1</sup>) without applying corrections for MSA contributions. To aid ease of comparison, all [S] has  
198 been converted to [SO<sub>4</sub><sup>2-</sup>], in the database and will be referred to only as [SO<sub>4</sub><sup>2-</sup>] in the data description.

199 **2.5. Flux vs concentration.**

200 [Na<sup>+</sup>] and [SO<sub>4</sub><sup>2-</sup>] in ice cores are generally reported as a concentration. Concentration can be converted to a  
201 deposition flux, provided that the snow accumulation rate is known. Flux (ppb kg m<sup>-2</sup>) = concentration (ppb) x  
202 snow accumulation (kg m<sup>-2</sup>). Snow accumulation records were extracted from the Antarctic regional snow  
203 accumulation composites available at the UK Polar data centre (Thomas, 2017). The CLIVASH2k database  
204 includes both concentrations and fluxes, when available. Flux estimates from ice cores combine both wet and  
205 dry deposition, of which the contribution of these two depositional modes varies across Antarctica with  
206 elevation and distance from the source (Wolff, 2012).  
207

208 **2.6. Establishing the sea salt and non-sea salt component.**

209 There are various methods of calculating the sea salt (ss) and excess (xs) components of an ice core chemistry  
210 record. The most-common method, as mentioned above, is to assume 100% of the [Na<sup>+</sup>] comes from the ocean.  
211 Then [Na<sup>+</sup>] can be treated as a marine reference species and the ss fraction of all other chemical species can be  
212 calculated based upon a mean ocean water elemental abundance reference value (e.g. (Lide, 2005)). If [Na<sup>+</sup>] is  
213 suspected of not being of marine origin, alternative methods of calculating the ss chemical fraction may be  
214 employed. For example, one may apply a standard sea-water ratio of 30.61 [Na<sup>+</sup>], 1.1 [K<sup>+</sup>], 3.69 [Mg<sup>2+</sup>], 1.16  
215 [Ca<sup>2+</sup>], 55.04 [Cl<sup>-</sup>] and 7.68 [SO<sub>4</sub><sup>2-</sup>] to the ion concentrations in each sample (Holland, 1978). Several studies  
216 have shown that frost flowers are depleted in [SO<sub>4</sub><sup>2-</sup>] relative to [Na<sup>+</sup>]. This produces a ssSO<sub>4</sub><sup>2-</sup> value which is  
217 slightly higher than it should be for sites near the coast (Rankin et al., 2002; Rankin et al., 2000). Unfortunately,  
218 not all studies accurately measure a wide suite of chemical species. Therefore, in this study we have assumed  
219 [Na<sup>+</sup>] to be the primary marine species and calculated xs [SO<sub>4</sub><sup>2-</sup>] according to the following ratio: [xsSO<sub>4</sub><sup>2-</sup>] =  
220 [SO<sub>4</sub><sup>2-</sup>] - 0.25[Na<sup>+</sup>] (O'Brien et al., 1995). Other ratios may be more suitable for coastal sites (Dixon et al.,  
221 2004), but for consistency we have applied the same ratio to all records reported in the database.

222

223 **2.7. Data validation and recommendations**

224 The two main uncertainties in the data presented arise from 1) chronological controls and 2) analytical errors.  
225 As discussed in section 2.2, all records have been synchronised to a common age-scale (WD2014). Thus, when  
226 using the entire database, we recommend using an error estimate of ±2 years, for records younger than 500

Formatted: Superscript

Formatted: Superscript

227 years, increasing to a conservative error estimate of  $\pm 5$  years for records extending to 2000 years. This is the  
 228 maximum uncertainty estimate for the WD2014 age-scale at 2,500 years (Sigl et al., 2015). However, we note  
 229 that for individual records in this database the published error estimates are as low as  $\pm 1$  year (e.g., Emanuelsson  
 230 et al., 2022). When using individual records we recommend using the published error estimate for that record.

231 Analytical precision varies between instruments and laboratories. We recommend applying a 1 standard error  
 232 ( $\sigma$ ) to the data to account for analytical errors.

233 The  $[\text{Na}^+]$  and  $[\text{SO}_4^{2-}]$  data is an accurate representation of either concentration or flux at a certain site.  
 234 However, how this relates to regional deposition is not well constrained. While we can account for the  
 235 uncertainty in analytical precision and dating error, we cannot define the signal to noise ratio associated with  
 236 small scale post-depositional process. For example, wind redistribution or the impact of local orography. The  
 237 regional climate and signal to local noise has been investigated for stable water isotopes in Antarctica (Münch  
 238 and Laepple, 2018) (e.g., Münch et al., 2018), however, a detailed investigation of  $[\text{Na}^+]$  and  $[\text{SO}_4^{2-}]$  is lacking.  
 239 One of the main limitations, which this database will address, has been the lack of available data. We thus  
 240 encourage database users to investigate the regional signal by averaging records to reduce the signal to noise  
 241 ratio. In this case, we recommend using the standard error propagation procedure for averaging for example the  
 242 square root of the sum of variances of individual records divided by the number of the records.

243 Ice cores provide the only record of  $[\text{Na}^+]$  and  $[\text{SO}_4^{2-}]$  deposition in Antarctica, and therefore, validation against  
 244 reference datasets is also not possible. While progress has been made using chemical transport models to  
 245 represent the deposition of sea salts in Greenland (Rhodes et al., 2018), the period examined is very short  
 246 (annual to decadal) and has currently not been applied to Antarctica. This database will provide much needed  
 247 data for any future model validation. However, currently it means there are no independent data products to  
 248 validate our  $[\text{Na}^+]$  and  $[\text{SO}_4^{2-}]$  records against.

249

### 250 3. Data records

251 A total of 117 records were submitted, representing 105 individual ice core sites (Fig. 1). In some locations,  
 252 duplicate analysis or updated versions were submitted (e.g. EPICA Dome C). This includes sites where  
 253 analysis was undertaken at different laboratories, using different instrumentation (e.g. IC and ICP-MS) or  
 254 different depth resolution. Some ice cores only provide data for a single species and not all records contain both  
 255 flux and concentration. A total of 94 ice core sites are included in the database which provide  $[\text{Na}^+]$ ,  $[\text{SO}_4^{2-}]$  and  
 256 xs  $[\text{SO}_4^{2-}]$ . All submitted records have been included in the database. The number of records submitted is  
 257 summarised in Table 1. The full list of records, their location, elevation, duration, and reference are presented in  
 258 appendix A (table A1S1).

259

260 **Table 1.** Summary of records submitted to the CLIVASH2k database. Combined records indicate sites which  
 261 contain all three species  $[\text{Na}^+]$ ,  $[\text{SO}_4^{2-}]$  and xs  $[\text{SO}_4^{2-}]$ .

262

263

264

	<u>Records submitted</u>	<u>Analytical replicates</u>	<u>Number of ice cores</u>
<u>Total records</u>	<u>117</u>	<u>12</u>	<u>105</u>
<u>Combined</u>	<u>97</u>	<u>3</u>	<u>94</u>
<u><math>[\text{Na}^+]</math></u>	<u>106</u>	<u>10</u>	<u>96</u>
<u><math>\text{Na}^+</math> flux</u>	<u>67</u>	<u>3</u>	<u>64</u>
<u><math>[\text{SO}_4^{2-}]</math></u>	<u>103</u>	<u>6</u>	<u>97</u>
<u><math>\text{SO}_4^{2-}</math> flux</u>	<u>64</u>	<u>3</u>	<u>61</u>
<u>xs <math>[\text{SO}_4^{2-}]</math></u>	<u>97</u>	<u>3</u>	<u>94</u>
<u>xs <math>\text{SO}_4^{2-}</math> flux</u>	<u>61</u>	<u>0</u>	<u>61</u>

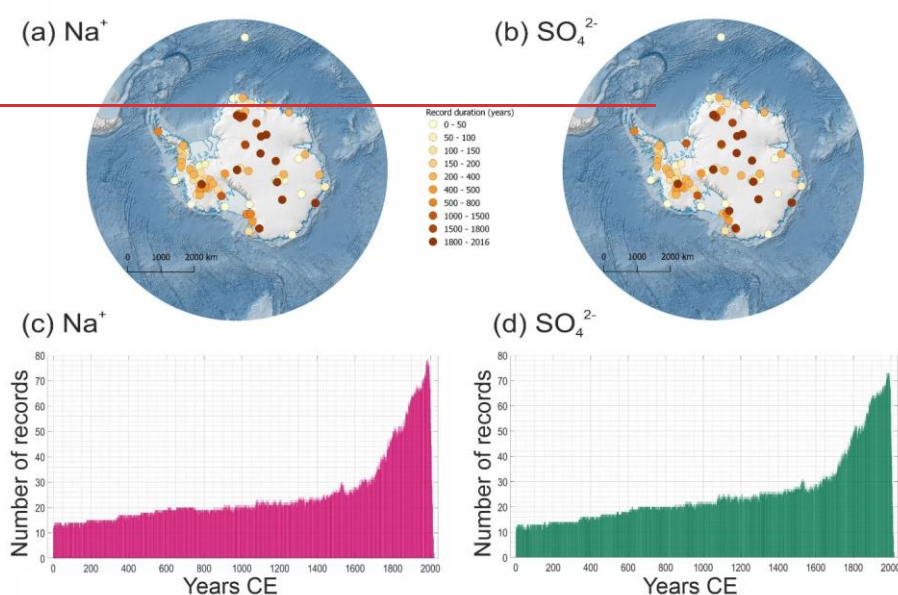
265

#### 266 3.1. Geographical and temporal coverage.

**Formatted:** Font: (Default) Times New Roman, 10 pt, Bold, Font color: Black  
**Formatted:** Normal, Indent: Left: 0 cm

267 There is reasonable spatial coverage across Antarctica, with the largest density of records in West Antarctica  
268 (Figs. 1a & 1b). In East Antarctica, notable data voids include Coats Land, Enderby and Kemp Land, Wilkes  
269 Land and Terra Adelie. There is a notable absence of long records from the Antarctic Peninsula. Despite the  
270 high density of records in West Antarctica, high snow accumulation in this region results in most of these  
271 records only spanning the last few decades or centuries.

272 The longer duration records (>1000 years) are predominantly found in the central East Antarctic plateau, while  
273 most higher snow accumulation coastal sites cover shorter timescales (Figs. 1a & 1b). The most recent year in  
274 the record peaks in the late 1990s, when the highest number of cores were drilled (Figs. 1c & 1d). Only eleven  
275 records span the full 2000 years.



276  
277 **Figure 1.** Spatial and temporal coverage of records in the CLIVASH2k database. Map of ice core locations with  
278 (a) [Na<sup>+</sup>], and (b) [SO<sub>4</sub><sup>2-</sup>] records. Colour coded based on record duration (number of years). The number of (c)  
279 [Na<sup>+</sup>] and (d) [SO<sub>4</sub><sup>2-</sup>] records as a function of the years (CE) covered.

### 280 3.1.1. Technical validation

281 To facilitate the scientific usability of this database, we have evaluated each record in terms of its relationship  
282 with key climate parameters during the observational period (1979- 2019). Given their varying temporal ranges  
283 (Fig. 1), not all the records span the full satellite period. Thus, correlations are based on the largest number of  
284 years available within this period. Although the database includes short records, for the data interpretation step,  
285 we have only included records that have at least ten years of overlap with the satellite and reanalysis climate  
286 data. Duplicate records (including updated versions and different analytical approaches) are included in the data  
287 interpretation step and interpreted as individual records.  
288

289 The objective of this climatological comparison is to provide a first level filter for the database. Based on the  
290 published literature (section 1) the deposition of [Na<sup>+</sup>] and [SO<sub>4</sub><sup>2-</sup>] has been linked to changes in sea ice, winds,  
291 and atmospheric circulation. Thus, these parameters have been chosen for the initial evaluation step.  
292 enabling database users to quickly search for sites that exhibit a direct and dynamically logical relationship with  
293 sea ice concentration (SIC), wind conditions and atmospheric circulation to facilitate future investigations.

294 All of the records were also correlated using ERA5 meteorological parameters (Hersbach et al., 2020), the fifth  
 295 generation European Centre for Medium Range Weather Forecast (ECMWF) atmospheric reanalysis data. These  
 296 parameters include 500-hPa geopotential height (Z500), meridional winds (v) and zonal winds (u) both at the  
 297 850-hPa level. The 850 hPa level was chosen to represent surface winds (relevant for sea ice reconstructions),  
 298 while the 500 hPa was chosen to capture larger-scale circulation across both high and low elevation sites. All  
 299 correlations were performed on de-trended annual average data (January – December) to correspond with the  
 300 annually-resolved ice core records and corrected for autocorrelation. All of the records were correlated with SIC  
 301 from the National Snow and Ice Data Centre (NSIDC) Nimbus-7 SMMR and DMSP SSM/I-SSMIS Passive  
 302 Microwave Data version 1 (Cavalieri et al., 1997).

303

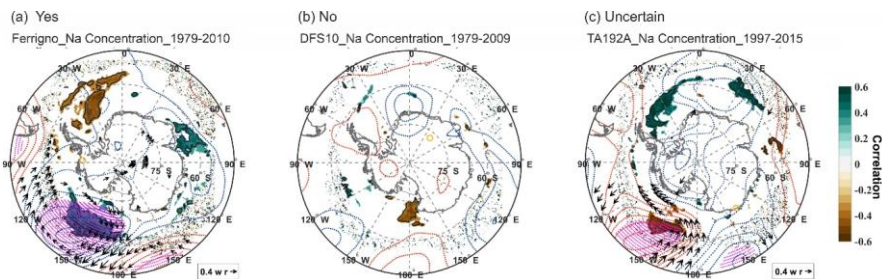
304

#### 305 4. Data interpretation

##### 306 4.1. Identifying sites that correlate with sea ice and atmospheric circulation

307 An example of the data interpretation output is presented in Figure 2. For consistency, correlations were  
 308 performed with climate variables across all longitudes in the southern hemisphere south of 50°S. This approach  
 309 has the potential to generate spurious results or correlations in regions that are physically unrelated to the site  
 310 (e.g., Fig. 2b). Indeed, studies have shown that climatic fields inherit patterns and correlations which can result  
 311 in statistically significant correlations by chance (Livezey and Chen, 1983). Therefore, each record was  
 312 individually evaluated by an expert (hereafter the “interpretation team”) to establish if the correlations observed  
 313 can be attributed to a realistic source region and transport mechanism. Sites with a clear connection or absence  
 314 of connection agreed by more than one interpreter were marked as either “yes” or “no” (Figs. 2a & 2b). Sites  
 315 where the transport mechanism was less clear, or there was a disagreement between interpreters were listed as  
 316 “uncertain” (Fig. 2c).

317



318

319 **Figure 2.** Example correlation plots evaluated by the data interpretation team. (a) Yes example, correlation  
 320 observed between all three parameters. (b) No example, no significant correlation observed with any parameters.  
 321 In this example, a significant correlation with SIC at a distant location is likely an auto-correlation artefact. (c)  
 322 Uncertain example, the transport mechanism could not be verified by the interpretation team. Yellow open circle  
 323 indicates ice core location. Coloured shading indicates positive (green) and negative (brown) correlations with  
 324 SIC (data from NSIDC), solid black line correlations significant at the 5% level. Correlations with winds  
 325 (arrows) composed of u850 and v850 (ERA 5). Dashed red and blue contours represent positive (red) and  
 326 negative (blue) correlations with geopotential height at 500 hPa (ERA5), pink hatching is significant at the 5%  
 327 level. Plot titles labelled as “Site name\_species\_years for correlation”.

328

329 In the following sections, we only refer to records that exhibited a correlation that is statistically significant at  
 330 the 5% level ( $p < 0.05$ ) (hereafter referred to as significant). For sites to be identified as having a relationship  
 331 with either SIC, atmospheric pressure (z500) or winds (u850 or v850), they had to be supported by a valid  
 332 transport mechanism or source region as evaluated by the data interpretation team (Fig. 2). We have not applied



333 a uniform cut-off size for the area of correlation or specified a minimum or maximum distance from the source  
 334 region, as these features will be site specific. For example, a low elevation coastal site (e.g., Sherman Island)  
 335 may only capture local changes in sea ice that will appear as a small area of correlation on the map (e.g.,  
 336 (Tetzner et al., 2021a) while a central Antarctic site (e.g., South Pole) might be influenced by long-range air-  
 337 masses and thus capture changes in sea ice from a relatively distant source region e.g., (Winski et al., 2021).

338 The database contains more concentration records than flux records. Thus, in the data interpretation we  
 339 presented both the total number of sites, and the proportion of sites, that exhibit a significant correlation with  
 340 meteorological parameters. The total number of eligible records for each species is shown in Table 3. The  
 341 spatial distribution of records is presented in figures 3, 4 and 5.

342

343 **Table 3.** Summary of the number of records that display a significant correlation (5% level) with SIC, wind  
 344 fields (meridional (v850) and zonal (u850)), and geopotential height (z500). The total records available for the  
 345 data interpretation step is shown for each species. This includes all records with more than 10-years overlap  
 346 with the instrumental period (1979-2018) and includes duplicates. Brackets indicate the number of sites marked  
 347 as “uncertain”. The percentage of records shown in italics underneath to account for the varying sample size.

348

Variable	[Na <sup>+</sup> ]	Na <sup>+</sup> Flux	[SO <sub>4</sub> <sup>2-</sup> ]	SO <sub>4</sub> <sup>2-</sup> Flux	xs [SO <sub>4</sub> <sup>2-</sup> ]	xs SO <sub>4</sub> <sup>2-</sup> Flux
Total records	88	65	84	61	81	59
SIC	69 (6) <i>78 %</i>	56 (4) <i>86 %</i>	60 (6) <i>71 %</i>	40 (5) <i>66 %</i>	68 (5) <i>84 %</i>	42 (2) <i>71 %</i>
Wind (v850 or u850)	63 (3) <i>72 %</i>	48 (4) <i>74 %</i>	54 (8) <i>64 %</i>	39 (3) <i>64 %</i>	56 (3) <i>69 %</i>	40 (3) <i>68 %</i>
Geopotential Height (z500)	47 (2) <i>53 %</i>	43 (3) <i>66 %</i>	38 (6) <i>45 %</i>	26 (3) <i>43 %</i>	40 (6) <i>49 %</i>	23 (3) <i>39 %</i>

349

350

#### 351 4.2. Sodium (concentration and flux)

352 A total of 69 (out of 88) [Na<sup>+</sup>] sites exhibit a correlation with SIC, with an additional six records marked as  
 353 “uncertain” (Table 3). Fifty-Six (out of 65) records are correlated with SIC when using Na<sup>+</sup> flux, with an  
 354 additional four sites marked as uncertain. This reflects the smaller number of flux records submitted to the  
 355 database. Proportionally, more records are correlated with SIC when using flux than concentration (78 %  
 356 compared to 72 %).

357

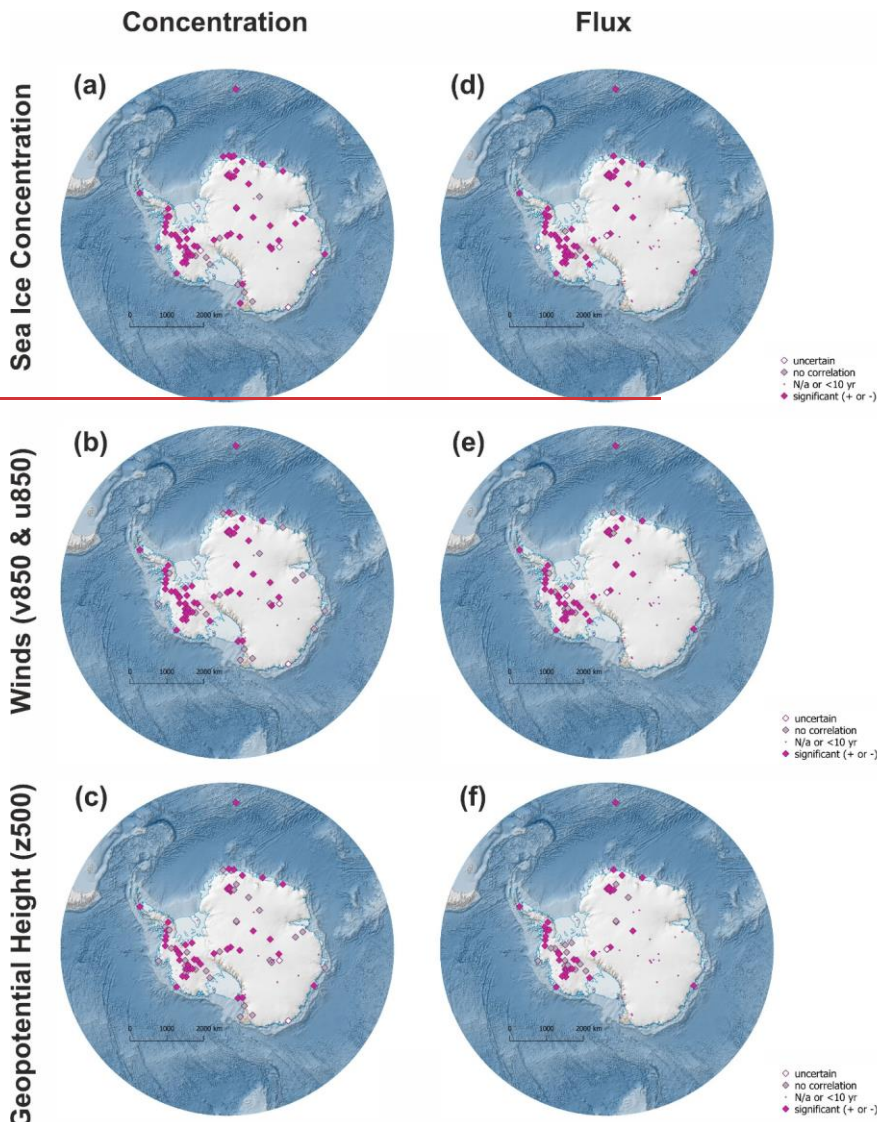
358 A total of 63 (out of 88) [Na<sup>+</sup>] records exhibit a significant correlation with the wind fields (v850 and u850).

359 While an additional ~~four~~three records were marked as uncertain. When using Na<sup>+</sup> flux 48 (out of 65) records  
 360 correlated with winds, with four records marked as uncertain. A higher proportion of records (74 % compared  
 361 with 72 %) correlated with winds when using flux.

362

363 A total of 47 (out of 88) [Na<sup>+</sup>] sites exhibit a significant correlation with geopotential height. While an  
 364 additional two records are marked as uncertain. The number of correlations with geopotential height is 43 (out  
 365 of 65) when using Na<sup>+</sup> flux, with an additional three sites marked as uncertain. A higher proportion of records  
 366 (66 % compared with 53 %) correlated with atmospheric circulation when using flux.

367



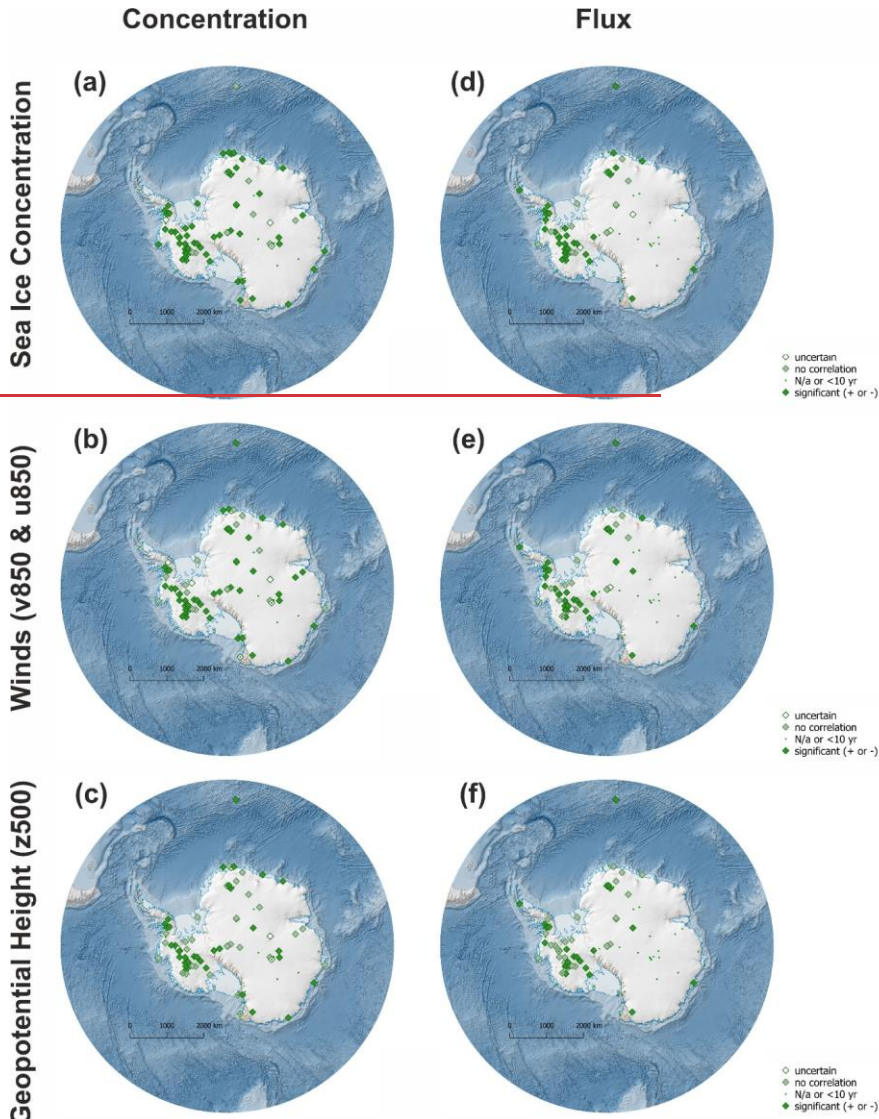
368  
 369  
 370 **Figure 3** – Geographical distribution of  $[Na^+]$  records (left column) which exhibit a statistically significant  
 371 ( $p > 0.05$ ) correlation with (a) SIC, (b) winds (v850 and u850) and (c) geopotential height (z500). Compared with  
 372 the geographical distribution of Na flux record (right column) which exhibit a statistically significant ( $p > 0.05$ )  
 373 correlation with (d) SIC, (e) winds (v850 and u850) and (f) geopotential height (z500). Pink diamonds are  
 374 locations with a significant correlation either positive or negative; grey diamonds are sites with no correlation,  
 375 open diamonds are uncertain. Dots indicate ice core locations that are in the database but either are less than 10  
 376 years in length (or overlap with the instrumental period) or sites which failed to generate any correlations with  
 377 parameters tested.  
 378  
 379

380 **4.3. Sulphate (concentration and flux)**

381 A total of 60 (out of 84) [SO<sub>4</sub><sup>2-</sup>] records display a correlation with SIC, with six additional records marked as  
382 uncertain (Table 3). When using SO<sub>4</sub><sup>2-</sup> flux, ~~39-40~~ (out of 61) records correlated with SIC, with an additional  
383 five records marked as uncertain. A slightly higher proportion of records (71 % compared with ~~64-66~~ %)   
384 correlated with SIC when using flux.

385 Fifty-four [SO<sub>4</sub><sup>2-</sup>] records (out of 84) are correlated with winds (v850 and u850), with eight additional records  
386 marked as uncertain. This is compared to 39 records (out of 61), and three additional records marked as  
387 uncertain, that are correlated with winds when using SO<sub>4</sub><sup>2-</sup> flux. The proportion of records correlated with winds  
388 (64 %) is the same when using either flux or concentration.

389 A total of 38 (out of 84) [SO<sub>4</sub><sup>2-</sup>] records are correlated with geopotential height, with six additional records  
390 marked as uncertain. This is compared with 26 records (out of ~~59-61~~) when using flux, with three marked as  
391 uncertain. A slightly higher proportion of records (45 % compared with 43 %) are correlated with atmospheric  
392 circulation when using flux.



393  
 394 **Figure 4** – Geographical distribution of  $[SO_4^{2-}]$  records (left column) which exhibit a statistically significant  
 395 ( $p > 0.05$ ) correlation with (a) SIC, (b) winds (v850 and u850) and (c) geopotential height (z500). Compared with  
 396 the geographical distribution of  $SO_4^{2-}$  flux record (right column) which exhibit a statistically significant ( $p > 0.05$ )  
 397 correlation with (d) SIC, (e) winds (v850 and u850) and (f) geopotential height (z500). Green diamonds are  
 398 locations with a significant correlation either positive or negative; grey diamonds are sites with no correlation,  
 399 open diamonds are uncertain. Dots indicate ice core locations that are in the database but either are less than 10  
 400 years in length (or overlap with the instrumental period) or sites which failed to generate any correlations with  
 401 parameters tested.

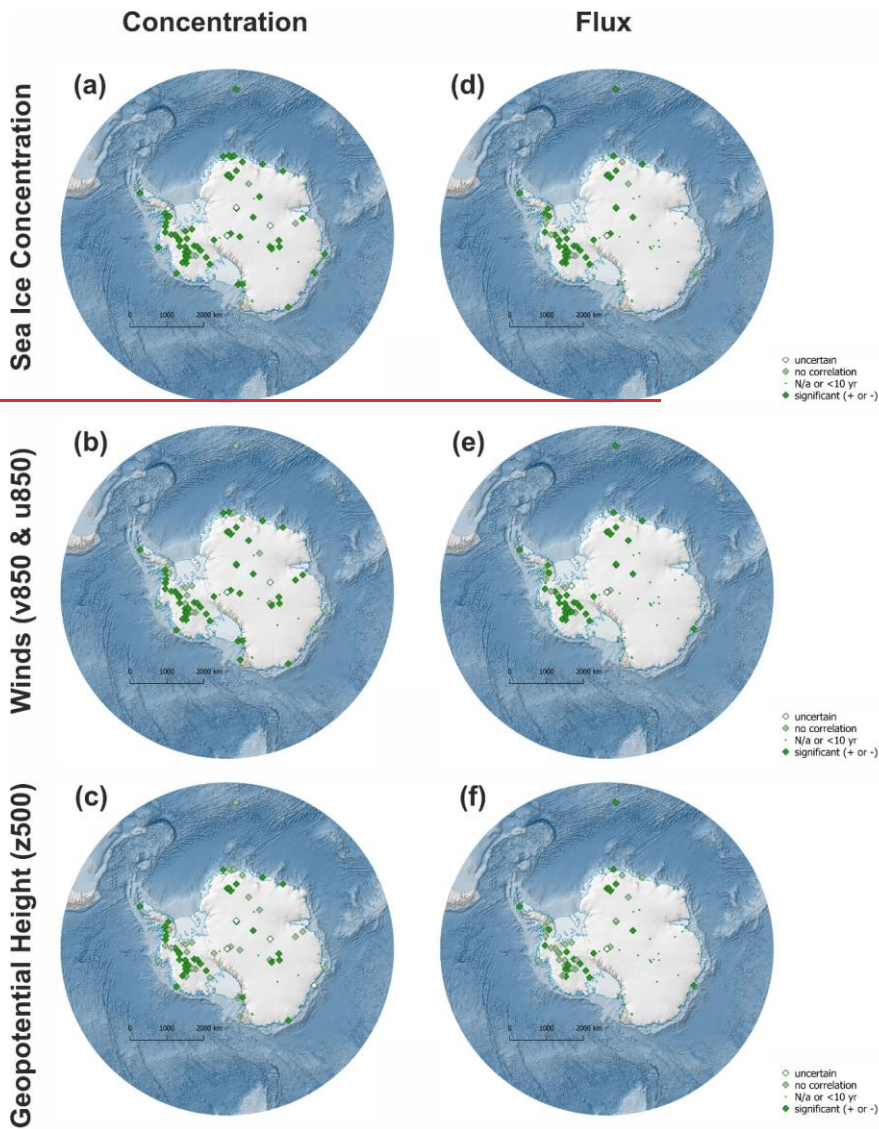
402

403 **4.4. Excess Sulphate (concentration and flux)**

404 A total of 68 (out of 81) xs [SO<sub>4</sub><sup>2-</sup>] records are correlated with SIC, with five additional records marked as  
405 uncertain when using concentration (Table 3). This number drops to 42 (out of 59) when using the flux, with  
406 two additional records marked as uncertain. A smaller proportion of records (71 % compared with 84 %)  
407 correlated with SIC when using flux.

408 A total of 56 (out of 81) xs [SO<sub>4</sub><sup>2-</sup>] records are correlated winds (v850 and u850), with three additional records  
409 marked as uncertain. The number drops to 40 (out of 59) records when using the xs SO<sub>4</sub><sup>2-</sup> flux, with three  
410 additional records marked as uncertain. A ~~smaller~~ ~~higher~~ proportion of records (~~68~~~~69~~% compared with ~~69~~~~68~~  
411 %) correlated with winds when using flux.

412 A total of 40 (out of 81) xs [SO<sub>4</sub><sup>2-</sup>] concentration records are correlated with geopotential height, with an  
413 additional six records marked as uncertain. The number drops to 23 (out of 59) records when using the xs SO<sub>4</sub><sup>2-</sup>  
414 flux, with three additional records marked as uncertain. A smaller proportion of records (39 % compared with  
415 49 %) correlated with atmospheric circulation when using flux.



416

417 **Figure 5** – Geographical distribution of xs  $[\text{SO}_4^{2-}]$  records (left column) which exhibit a statistically significant  
 418 ( $p>0.05$ ) correlation with (a) SIC, (b) winds (v850 and u850) and (c) geopotential height (z500). Compared with  
 419 the geographical distribution of xs  $\text{SO}_4^{2-}$  flux record (right column) which exhibit a statistically significant  
 420 ( $p>0.05$ ) correlation with (d) SIC, (e) winds (v850 and u850) and (f) geopotential height (z500). Green  
 421 diamonds are locations with a significant correlation either positive or negative; grey diamonds are sites with no  
 422 correlation, open diamonds are uncertain. Dots indicate ice core locations that are in the database but either are  
 423 less than 10 years in length (or overlap with the instrumental period) or sites which failed to generate any  
 424 correlations with parameters tested.

425

## 426 5. Discussion

### 427 5.1. Which records are suitable for reconstructing SIC, winds and atmospheric circulation?

428 Our findings reveal that  $[\text{Na}^+]$  provides the highest number (69) of records that exhibit a significant correlation  
429 with SIC. Only fractionally higher than the number of xs  $[\text{SO}_4^{2-}]$  records (68) and SO4 (60). ~~Thus, it suggests~~  
430 ~~that~~ all three records have the potential to capture changes in sea ice conditions. The full list of which sites  
431 exhibit positive correlations with each parameter is shown in Supplementary Figure S2.

432  $[\text{Na}^+]$  also provides the highest number of correlations with geopotential height (47) and wind (63). However,  
433 proportionally Na flux has the highest number of correlations with geopotential height and winds. While less  
434 than 49% of the  $[\text{SO}_4^{2-}]$  and xs  $[\text{SO}_4^{2-}]$  data exhibit relationships with geopotential height, a much higher  
435 percentage (64-69 %) display correlations with winds. This suggests that there is greater potential for using  
436  $[\text{SO}_4^{2-}]$  and xs  $[\text{SO}_4^{2-}]$  for reconstructing winds and SIC than geopotential heights. Removing the sea-salt  
437 component of  $[\text{SO}_4^{2-}]$  to produce xs  $[\text{SO}_4^{2-}]$  improves the relationship with SIC, geopotential height and winds.

438 Most of the records from West Antarctica and the Antarctic Peninsula (both  $[\text{Na}^+]$  and  $[\text{SO}_4^{2-}]$ ) exhibit  
439 correlations with SIC, geopotential height and winds. This reflects the dominance of marine air-mass incursions  
440 in this region (Suzuki et al., 2013), transporting sea salt aerosols from the sea ice zone to the ice core sites. In  
441 ~~contrast, in~~ East Antarctica, the high elevation of the ice sheet (>3000 m) acts as a barrier to marine air-mass  
442 transport. However, this study corroborates previous studies (e.g., (Winski et al., 2021)) suggesting that  $[\text{Na}^+]$   
443 and  $[\text{SO}_4^{2-}]$  concentrations from ice cores in the East Antarctic plateau are significantly correlated with SIC and  
444 atmospheric circulation.

445 Converting the records to flux drastically reduces the geographical coverage. In most cases this is due to the lack  
446 of available snow accumulation records from central Antarctica ~~to convert to~~ needed to calculate the flux.  
447 However, our study demonstrates that converting  $[\text{Na}^+]$  to flux increases the relative proportion of records that  
448 exhibit a significant correlation with SIC, geopotential height and winds. The opposite is true for  $[\text{SO}_4^{2-}]$  and xs  
449  $[\text{SO}_4^{2-}]$ , which results in a lower proportion of records correlating with SIC after converting to flux. This may  
450 suggest a dominance of wet deposition of  $[\text{Na}^+]$  and dry deposition of  $[\text{SO}_4^{2-}]$ . However, a detailed evaluation of  
451 the relationships between ion concentration and snow accumulation is needed to address this fully.

452 Overall, ~~the records of~~  $[\text{Na}^+]$  ~~provides the most records which exhibit significant correlations across all three~~  
453 ~~parameters exhibit the highest number of correlations with the climatic variables considered~~ (179 out of 264),  
454 followed by xs  $[\text{SO}_4^{2-}]$  (164 out of 243) and  $[\text{SO}_4^{2-}]$  (152 out of 252).

### 455 5.2. Potential limitations

456 There are limitations to this assessment, which is intended as a first pass filter to highlight the potential future  
457 use of the data. In particular, the numbers only relate to records that span or have at least 10-years of data that  
458 overlap with the instrumental period. This is defined as the period from 1979-2019 and accounts for 88% of the  
459 records (438 out of 499 records submitted). Thus, relationships may exist for shorter records or records drilled  
460 prior to 1979, however, it is not possible to verify this under the defined criteria. Another caveat is that  
461 correlations have only been conducted with a single sea ice (NSIDC) and reanalysis (ERA-5) product, and  
462 results may vary with different datasets. Results may also be impacted by the different timespans used. For  
463 example, it was not possible to select the same reference period to run all correlations, because record lengths  
464 and top ages (date the core was drilled) vary considerably. Thus, the assumed stationarity in the source and  
465 transport routes may not be appropriate.

466 We also note that almost 8% of the records have been classified as “uncertain”. In some cases, significant  
467 correlations were evident in the plots, but they were difficult to explain (Fig. 2c). For example, Law Dome  
468 generates several regions of significant correlations across multiple sectors, however not in the ocean adjacent to  
469 the site. This may indicate long-term transport or the influence of large-scale atmospheric circulation (e.g.,  
470 SAM, Indian Ocean Dipole, Atlantic Multidecadal Oscillation). However, in this first pass filter we only  
471 included sites where a clear mechanism was evident.

472

## 473 6. Data availability

474 This data descriptor presents version 1.0.0 of the CLIVASH2k Antarctic ice core chemistry database PAGES  
475 CLIVASH2k database (Thomas et al., 2022). The database can be accessed via the UK Polar Data Centre.  
476 NERC EDS UK Polar Data Centre. <https://doi.org/10.5285/9E0ED16E-F2AB-4372-8DF3-FDE7E388C9A7>

477

## 478 7. Conclusions.

479 The CLIVASH2k database is the first attempt to compile an Antarctic continental-scale database of chemical  
480 records in ice cores spanning the past 2000 years. This study is the first phase of the project, the goal of which  
481 was to compile and publish the records. In this study we have provided all available  $[\text{Na}^+]$  and  $[\text{SO}_4^{2-}]$  records  
482 submitted by the community. The records are all available as annual averages, included as both concentration  
483 and flux (if available). An additional parameter, xs  $[\text{SO}_4^{2-}]$  has also been calculated where possible.

484 To facilitate future data interpretation, we have run spatial correlations for all the records. The aim of this  
485 analysis is to identify sites which exhibit a statistically significant relationship with sea ice concentration (SIC)  
486 and atmospheric circulation (500-hPa geopotential heights) or winds (v850 and u850). This is intended as a first  
487 filter to identify potential records that could be used in future proxy reconstructions.

488 This first pass filter demonstrates that when considering the species separately, 335 individual records exhibit  
489 statistically significant correlations with SIC that have been verified by a team of experts. A recent compilation  
490 of available ice core derived sea ice reconstructions, based on a range of proxy data, identified only 17  
491 individual sites which have been used to reconstruct sea ice (Thomas et al., 2019). Thus, this data compilation  
492 represents a significant improvement on existing published or available data.

493 For researchers interested in reconstructing winds or atmospheric circulation the CLIVASH2k database contains  
494 a total of 300 records that are significantly correlated with the wind fields (v850 and u850) and 217 records that  
495 are significantly correlated with geopotential height (500 hPa). The  $\text{Na}^+$  flux exhibits the greatest proportion of  
496 records that correlate with sea ice, atmospheric circulation, and winds. Therefore, among the ice-core chemical  
497 species considered in our analysis, we propose  $\text{Na}^+$  flux may be the best proxy for  
498 reconstructing all three parameters as the best candidate for reconstructing all three climatic components.

499 Future work will focus on using this database to:

- 500 1) Investigate the deposition of  $[\text{Na}^+]$  and  $[\text{SO}_4^{2-}]$  over decadal to centennial timescales.
- 501 2) Provide a reconstruction of sea ice or atmospheric circulation spanning the past 2000 years.
- 502 3) Evaluate the skill of chemical transport models to capture observed deposition of  $[\text{Na}^+]$  and  $[\text{SO}_4^{2-}]$ .
- 503 4) Combine the information in this new database with the database of snow accumulation (Thomas et al.,  
504 2017) and isotopic content (Stenni et al., 2017) to obtain a comprehensive view of Antarctic climate  
505 variations over the past 2000 years.

506 This is not an exhaustive list, and we encourage the community to engage with the CLIVASH2k working group  
507 and make use of the database.

508

## 509 Author contributions

510 ET and HG conceived the idea. ET & DV initiated the data call and coordinated the project. ET wrote the paper  
511 with contributions from the core writing group. The core writing group (DV, ACFK, DE, HG, DW, VHLW,  
512 DD, DU, TV), contributed to the paper writing and discussions. The data interpretation team (ET, DV, ACFK,  
513 DW, VHLW, DD, NC, DU, TV, DT, MMG, MS) quality checked the data, evaluated the age-scales, and  
514 interpreted the spatial correlation plots. NANB, AH, CML, JRM, YM, KT, HM, YN, FS, JCS, MS, RT, SW,  
515 CX, JY, TVK, AAE, LPG and EMT all provided unpublished data. DE wrote the code for the data interpretation  
516 plots. DV & LT compiled the figures. All authors read and commented on the manuscript.

517 The following researchers contributed published data to this database. Yoshiyuki Fujii, Lenneke Jong, Elisabeth  
518 Isaksson, Filipe G. L. Lindau, Andrew Moy, Rachael Rhodes. We thank the many other researchers who have  
519 already made their data available on public data repositories.

## 520 Competing interests



521 The authors declare no competing conflict of interest.

## 522 Acknowledgements

523 CLIVASH2k is a contribution of Phase 3 of the PAGES 2k network. DT was funded as part of the PAGES Data  
524 Stewardship scholarship awarded to ET. This financial support comes from the Chinese Academy of Sciences  
525 (CAS) and the Swiss Academy of Sciences (SCNAT). We thank the PAGES office for their support and the  
526 temporary data storage during the compilation of this database.

## 527 References

- 528 Arienzo, M. M., McConnell, J. R., Chellman, N., and Kipfstuhl, S.: Method for Correcting Continuous Ice-Core  
529 Elemental Measurements for Under-Recovery, *Environmental Science & Technology*, 53, 5887-5894,  
530 10.1021/acs.est.9b00199, 2019.
- 531 Barnes, I., Hjorth, J., and Mihalopoulos, N.: Dimethyl Sulfoxide and Dimethyl Sulfoxide and Their Oxidation in  
532 the Atmosphere, *Chemical Reviews*, 106, 940-975, 10.1021/cr020529+, 2006.
- 533 Brean, J., Dall'Osto, M., Simó, R., Shi, Z., Beddows, D. C. S., and Harrison, R. M.: Open ocean and coastal  
534 new particle formation from sulfuric acid and amines around the Antarctic Peninsula, *Nature*  
535 *Geoscience*, 14, 383-388, 10.1038/s41561-021-00751-y, 2021.
- 536 Büntgen, U., Wacker, L., Galván, J. D., Arnold, S., Arseneault, D., Baillie, M., Beer, J., Bernabei, M., Bleicher,  
537 N., Boswijk, G., Bräuning, A., Carrer, M., Ljungqvist, F. C., Cherubini, P., Christl, M., Christie, D. A.,  
538 Clark, P. W., Cook, E. R., D'Arrigo, R., Davi, N., Eggertsson, O., Esper, J., Fowler, A. M., Gedalof, Z.  
539 e., Gennaretti, F., Griebinger, J., Grissino-Mayer, H., Grudd, H., Gunnarson, B. E., Hantemirov, R.,  
540 Herzig, F., Hessel, A., Heussner, K.-U., Jull, A. J. T., Kukarskih, V., Kirilyanov, A., Kolář, T., Krusic,  
541 P. J., Kyncl, T., Lara, A., LeQuesne, C., Linderholm, H. W., Loader, N. J., Luckman, B., Miyake, F.,  
542 Myglan, V. S., Nicolussi, K., Oppenheimer, C., Palmer, J., Panyushkina, I., Pederson, N., Rybníček,  
543 M., Schweingruber, F. H., Seim, A., Sigl, M., Churakova, O., Speer, J. H., Synal, H.-A., Tegel, W.,  
544 Treyde, K., Villalba, R., Wiles, G., Wilson, R., Winship, L. J., Wunder, J., Yang, B., and Young, G. H.  
545 F.: Tree rings reveal globally coherent signature of cosmogenic radiocarbon events in 774 and 993 CE,  
546 *Nature Communications*, 9, 3605, 10.1038/s41467-018-06036-0, 2018.
- 547 Cavalieri, D. J., Gloersen, P., Parkinson, C. L., Comiso, J. C., and Zwally, H. J.: Observed hemispheric  
548 asymmetry in global sea ice changes, *Science*, 278, 1104-1106, 1997.
- 549 Cole-Dai, J., Ferris, D. G., Kennedy, J. A., Sigl, M., McConnell, J. R., Fudge, T. J., Geng, L., Maselli, O. J.,  
550 Taylor, K. C., and Souney, J. M.: Comprehensive Record of Volcanic Eruptions in the Holocene  
551 (11,000 years) From the WAIS Divide, Antarctica Ice Core, *Journal of Geophysical Research:  
552 Atmospheres*, 126, e2020JD032855, <https://doi.org/10.1029/2020JD032855>, 2021.
- 553 Dalaiden, Q., Goosse, H., Rezsöhazy, J., and Thomas, E. R.: Reconstructing atmospheric circulation and sea-ice  
554 extent in the West Antarctic over the past 200 years using data assimilation, *Climate Dynamics*,  
555 10.1007/s00382-021-05879-6, 2021.
- 556 Delmas, R., Briat, M., and Legrand, M.: Chemistry of south polar snow, *Journal of Geophysical Research:  
557 Oceans*, 87, 4314-4318, <https://doi.org/10.1029/JC087iC06p04314>, 1982.
- 558 Dixon, D., Mayewski, P. A., Kaspari, S., Sneed, S., and Handley, M.: A 200 year sub-annual record of sulfate in  
559 West Antarctica, from 16 ice cores, *Annals of Glaciology*, 39, 545-556,  
560 10.3189/172756404781814113, 2004.
- 561 Ekaykin, A. A., Kozachek, A. V., Lipenkov, V. Y., and Shibaev, Y. A.: Multiple climate shifts in the Southern  
562 Hemisphere over the past three centuries based on central Antarctic snow pits and core studies, *Annals  
563 of Glaciology*, 55, 259-266, 10.3189/2014AoG66A189, 2014.
- 564 Emanuelsson, B. D., Thomas, E. R., Tetzner, D. R., Humby, J. D., and Vladimirova, D. O.: Ice Core  
565 Chronologies from the Antarctic Peninsula: The Palmer, Jurassic, and Rendezvous Age-Scales,  
566 *Geosciences*, 12, 87, 2022.
- 567 Fogt, R. L., Sleinkofer, A. M., Raphael, M. N., and Handcock, M. S.: A regime shift in seasonal total Antarctic  
568 sea ice extent in the twentieth century, *Nature Climate Change*, 12, 54-62, 10.1038/s41558-021-01254-  
569 9, 2022.
- 570 Frey, M. M., Norris, S. J., Brooks, I. M., Anderson, P. S., Nishimura, K., Yang, X., Jones, A. E., Nerentorp  
571 Mastromonaco, M. G., Jones, D. H., and Wolff, E. W.: First direct observation of sea salt aerosol  
572 production from blowing snow above sea ice, *Atmospheric Chemistry and Physics*, 20, 2549-2578,  
573 2020.
- 574 Gondwe, M., Krol, M., Gieskes, W., Klaassen, W., and de Baar, H.: The contribution of ocean-leaving DMS to  
575 the global atmospheric burdens of DMS, MSA, SO<sub>2</sub>, and NSS SO<sub>4</sub><sup>=</sup>, *Global Biogeochemical Cycles*,  
576 17, <https://doi.org/10.1029/2002GB001937>, 2003.

Formatted: Font: (Default) Times New Roman, 10 pt

Formatted: Indent Left: 0 cm, Hanging: 1.27 cm

Formatted: Font: (Default) Times New Roman, 10 pt

Formatted: Font: (Default) Times New Roman, 10 pt

Formatted: Font: (Default) Times New Roman, 10 pt

Formatted: Font: (Default) Times New Roman, 10 pt

Formatted: Font: (Default) Times New Roman, 10 pt

Formatted: Font: (Default) Times New Roman, 10 pt

577 Grieman, M. M., Hoffmann, H. M., Humby, J. D., Mulvaney, R., Nehrass-Ahles, C., Rix, J., Thomas, E. R.,  
578 Tuckwell, R., and Wolff, E. W.: Continuous flow analysis methods for sodium, magnesium and  
579 calcium detection in the Skytrain ice core, *Journal of Glaciology*, 68, 90-100, 10.1017/jog.2021.75,  
580 2022.

581 Hersbach, H., Bell, B., Berrisford, P., Hirahara, S., Horányi, A., Muñoz-Sabater, J., Nicolas, J., Peubey, C.,  
582 Radu, R., and Schepers, D.: The ERA5 global reanalysis, *Quarterly Journal of the Royal  
583 Meteorological Society*, 146, 1999-2049, 2020.

584 Holland, H. D.: *The chemistry of the atmosphere and oceans*, 1978.

585 Huang, J. and Jaeglé, L.: Wintertime enhancements of sea salt aerosol in polar regions consistent with a sea ice  
586 source from blowing snow, *Atmos. Chem. Phys.*, 17, 3699-3712, 10.5194/acp-17-3699-2017, 2017.

587 Jones, J. M., Gille, S. T., Goosse, H., Abram, N. J., Canziani, P. O., Charman, D. J., Clem, K. R., Crosta, X., de  
588 Lavergne, C., Eisenman, I., England, M. H., Fogt, R. L., Frankcombe, L. M., Marshall, G. J., Masson-  
589 Delmotte, V., Morrison, A. K., Orsi, A. J., Raphael, M. N., Renwick, J. A., Schneider, D. P., Simpkins,  
590 G. R., Steig, E. J., Stenni, B., Swingedouw, D., and Vance, T. R.: Assessing recent trends in high-  
591 latitude Southern Hemisphere surface climate, *Nature Climate Change*, 6, 917-926,  
592 10.1038/nclimate3103, 2016.

593 Jungclaus, J. H., Bard, E., Baroni, M., Braconnot, P., Cao, J., Chini, L. P., Egorova, T., Evans, M., González-  
594 Rouco, J. F., Goosse, H., Hurrell, G. C., Joos, F., Kaplan, J. O., Khodri, M., Klein Goldewijk, K.,  
595 Krivova, N., LeGrande, A. N., Lorenz, S. J., Luterbacher, J., Man, W., Maycock, A. C., Meinshausen,  
596 M., Moberg, A., Muscheler, R., Nehrass-Ahles, C., Otto-Bliesner, B. I., Phipps, S. J., Pongratz, J.,  
597 Rozanov, E., Schmidt, G. A., Schmidt, H., Schmutz, W., Schurer, A., Shapiro, A. I., Sigl, M.,  
598 Smerdon, J. E., Solanki, S. K., Timmreck, C., Toohey, M., Usoskin, I. G., Wagner, S., Wu, C. J., Yeo,  
599 K. L., Zanchettin, D., Zhang, Q., and Zorita, E.: The PMIP4 contribution to CMIP6 – Part 3: The last  
600 millennium, scientific objective, and experimental design for the PMIP4 past1000 simulations, *Geosci.  
601 Model Dev.*, 10, 4005-4033, 10.5194/gmd-10-4005-2017, 2017.

602 Kaufman, D., McKay, N., Routson, C., Erb, M., Dätwyler, C., Sommer, P. S., Heiri, O., and Davis, B.:  
603 Holocene global mean surface temperature, a multi-method reconstruction approach, *Scientific Data*, 7,  
604 201, 10.1038/s41597-020-0530-7, 2020.

605 Konecky, B. L., McKay, N. P., Churakova, O. V., Comas-Bru, L., Dassié, E. P., DeLong, K. L., Falster, G. M.,  
606 Fischer, M. J., Jones, M. D., Jonkers, L., Kaufman, D. S., Leduc, G., Managave, S. R., Martrat, B.,  
607 Opel, T., Orsi, A. J., Partin, J. W., Sayani, H. R., Thomas, E. K., Thompson, D. M., Tyler, J. J., Abram,  
608 N. J., Atwood, A. R., Cartapanis, O., Conroy, J. L., Curran, M. A., Dee, S. G., Deininger, M., Divine,  
609 D. V., Kern, Z., Porter, T. J., Stevenson, S. L., von Gunten, L., and Iso2k Project, M.: The Iso2k  
610 database: a global compilation of paleo- $\delta^{18}O$  and  $\delta^2H$  records to aid understanding of Common Era  
611 climate, *Earth Syst. Sci. Data*, 12, 2261-2288, 10.5194/essd-12-2261-2020, 2020.

612 Legrand, M. and Mayewski, P.: Glaciochemistry of polar ice cores: A review, *Reviews of Geophysics*, 35, 219-  
613 243, <https://doi.org/10.1029/96RG03527>, 1997.

614 Legrand, M., Feniet-Saigne, C., Saltzman, E. S., and Germain, C.: Spatial and temporal variations of  
615 methanesulfonic acid and non sea salt sulfate in Antarctic ice, *Journal of Atmospheric Chemistry*, 14,  
616 245-260, 10.1007/BF00115237, 1992.

617 Lide, D.: *CRC Handbook of Chemistry and Physics*, Internet Version 2005 CRC Press, Boca Raton, FL, 2005.

618 Livezey, R. E. and Chen, W.: Statistical field significance and its determination by Monte Carlo techniques,  
619 *Mon. Wea. Rev.*, 111, 46-59, 1983.

620 Mayewski, P. A., Carleton, A. M., Birkel, S. D., Dixon, D., Kurbatov, A. V., Korotkikh, E., McConnell, J.,  
621 Curran, M., Cole-Dai, J., Jiang, S., Plummer, C., Vance, T., Maasch, K. A., Sneed, S. B., and Handley,  
622 M.: Ice core and climate reanalysis analogs to predict Antarctic and Southern Hemisphere climate  
623 changes, *Quaternary Science Reviews*, 155, 50-66, <https://doi.org/10.1016/j.quascirev.2016.11.017>,  
624 2017.

625 McCoy, D. T., Burrows, S. M., Wood, R., Grosvenor, D. P., Elliott, S. M., Ma, P.-L., Rasch, P. J., and  
626 Hartmann, D. L.: Natural aerosols explain seasonal and spatial patterns of Southern Ocean cloud  
627 albedo, *Science Advances*, 1, e1500157, doi:10.1126/sciadv.1500157, 2015.

628 McGregor, H. V., Evans, M. N., Goosse, H., Leduc, G., Martrat, B., Addison, J. A., Mortyn, P. G., Oppo, D.  
629 W., Seidenkrantz, M.-S., Sicre, M.-A., Phipps, S. J., Selvaraj, K., Thirumalai, K., Filipsson, H. L., and  
630 Ersek, V.: Robust global ocean cooling trend for the pre-industrial Common Era, *Nature Geoscience*, 8,  
631 671-677, 10.1038/ngeo2510, 2015.

632 McKay, N. P. and Kaufman, D. S.: An extended Arctic proxy temperature database for the past 2,000 years,  
633 *Scientific Data*, 1, 140026, 10.1038/sdata.2014.26, 2014.

634 Medley, B. and Thomas, E. R.: Increased snowfall over the Antarctic Ice Sheet mitigated twentieth-century sea-  
635 level rise, *Nature Climate Change*, 9, 34-39, 10.1038/s41558-018-0356-x, 2019.

Formatted: Font (Default) Times New Roman, 10 pt

Formatted: Font (Default) Times New Roman, 10 pt

Formatted: Font (Default) Times New Roman, 10 pt

Formatted: Font (Default) Times New Roman, 10 pt

636 Meehl, G. A., Arblaster, J. M., Bitz, C. M., Chung, C. T. Y., and Teng, H.: Antarctic sea-ice expansion between  
637 2000 and 2014 driven by tropical Pacific decadal climate variability, *Nature Geoscience*, 9, 590-595,  
638 10.1038/ngeo2751, 2016.

639 Minikin, A., Wagenbach, D., Graf, W., and Kipfstuhl, J.: Spatial and seasonal variations of the snow chemistry  
640 at the central Filchner-Ronne Ice Shelf, Antarctica, *Annals of Glaciology*, 20, 283-290, 1994.

641 Münch, T. and Laepple, T.: What climate signal is contained in decadal- to centennial-scale isotope variations  
642 from Antarctic ice cores?, *Clim. Past*, 14, 2053-2070, 10.5194/cp-14-2053-2018, 2018.

643 O'Brien, S. R., Mayewski, P. A., Meeker, L. D., Meese, D. A., Twickler, M. S., and Whitlow, S. I.: Complexity  
644 of Holocene Climate as Reconstructed from a Greenland Ice Core, *Science*, 270, 1962-1964,  
645 doi:10.1126/science.270.5244.1962, 1995.

646 Plummer, C. T., Curran, M. A. J., van Ommen, T. D., Rasmussen, S. O., Moy, A. D., Vance, T. R., Clausen, H.  
647 B., Vinther, B. M., and Mayewski, P. A.: An independently dated 2000-yr volcanic record from Law  
648 Dome, East Antarctica, including a new perspective on the dating of the 1450s CE eruption of Kuwae,  
649 Vanuatu, *Clim. Past*, 8, 1929-1940, 10.5194/cp-8-1929-2012, 2012.

650 Rankin, A. M., Auld, V., and Wolff, E. W.: Frost flowers as a source of fractionated sea salt aerosol in the polar  
651 regions, *Geophysical Research Letters*, 27, 3469-3472, 10.1029/2000gl011771, 2000.

652 Rankin, A. M., Wolff, E. W., and Martin, S.: Frost flowers: Implications for tropospheric chemistry and ice core  
653 interpretation, *Journal of Geophysical Research: Atmospheres*, 107, AAC 4-1-AAC 4-15,  
654 10.1029/2002jd002492, 2002.

655 Ren, J., Li, C., Hou, S., Xiao, C., Qin, D., Li, Y., and Ding, M.: A 2680 year volcanic record from the DT-401  
656 East Antarctic ice core, *Journal of Geophysical Research: Atmospheres*, 115,  
657 <https://doi.org/10.1029/2009JD012892>, 2010.

658 Rhodes, R. H., Yang, X., and Wolff, E. W.: Sea Ice Versus Storms: What Controls Sea Salt in Arctic Ice Cores?,  
659 *Geophysical Research Letters*, 45, 5572-5580, 10.1029/2018gl077403, 2018.

660 Roach, L. A., Dörr, J., Holmes, C. R., Massonnet, F., Blockley, E. W., Notz, D., Rackow, T., Raphael, M. N.,  
661 O'Farrell, S. P., Bailey, D. A., and Bitz, C. M.: Antarctic Sea Ice Area in CMIP6, *Geophysical  
662 Research Letters*, 47, e2019GL086729, <https://doi.org/10.1029/2019GL086729>, 2020.

663 Saltzman, E. S., Dioumaeva, I., and Finley, B. D.: Glacial/interglacial variations in methanesulfonate (MSA) in  
664 the Siple Dome ice core, West Antarctica, *Geophysical Research Letters*, 33,  
665 <https://doi.org/10.1029/2005GL025629>, 2006.

666 Severi, M., Becagli, S., Caiazza, L., Ciardini, V., Colizza, E., Giardi, F., Mezgec, K., Scarchilli, C., Stenni, B.,  
667 Thomas, E. R., Traversi, R., and Udisti, R.: Sea salt sodium record from Talos Dome (East Antarctica)  
668 as a potential proxy of the Antarctic past sea ice extent, *Chemosphere*, 177, 266-274,  
669 <https://doi.org/10.1016/j.chemosphere.2017.03.025>, 2017.

670 Sigl, M., McConnell, J. R., Toohey, M., Curran, M., Das, S. B., Edwards, R., Isaksson, E., Kawamura, K.,  
671 Kipfstuhl, S., Krüger, K., Layman, L., Maselli, O. J., Motizuki, Y., Motoyama, H., Pasteris, D. R., and  
672 Severi, M.: Insights from Antarctica on volcanic forcing during the Common Era, *Nature Climate  
673 Change*, 4, 693-697, 10.1038/nclimate2293, 2014.

674 Sigl, M., Winstrup, M., McConnell, J. R., Welten, K. C., Plunkett, G., Ludlow, F., Büntgen, U., Caffee, M.,  
675 Chellman, N., Dahl-Jensen, D., Fischer, H., Kipfstuhl, S., Kostick, C., Maselli, O. J., Mekhaldi, F.,  
676 Mulvaney, R., Muscheler, R., Pasteris, D. R., Pilcher, J. R., Salzer, M., Schüpbach, S., Steffensen, J. P.,  
677 Vinther, B. M., and Woodruff, T. E.: Timing and climate forcing of volcanic eruptions for the past  
678 2,500 years, *Nature*, 523, 543-549, 10.1038/nature14565, 2015.

679 Sigl, M., Fudge, T. J., Winstrup, M., Cole-Dai, J., Ferris, D., McConnell, J. R., Taylor, K. C., Welten, K. C.,  
680 Woodruff, T. E., Adolphi, F., Bisiaux, M., Brook, E. J., Buizert, C., Caffee, M. W., Dunbar, N. W.,  
681 Edwards, R., Geng, L., Iverson, N., Koffman, B., Layman, L., Maselli, O. J., McGwire, K., Muscheler,  
682 R., Nishiizumi, K., Pasteris, D. R., Rhodes, R. H., and Sowers, T. A.: The WAIS Divide deep ice core  
683 WD2014 chronology – Part 2: Annual-layer counting (0–31 ka BP), *Clim. Past*, 12, 769-786,  
684 10.5194/cp-12-769-2016, 2016.

685 Sneed, S. B., Mayewski, P. A., and Dixon, D. A.: An emerging technique: multi-ice-core multi-parameter  
686 correlations with Antarctic sea-ice extent, *Annals of Glaciology*, 52, 347-354,  
687 10.3189/172756411795931822, 2011.

688 Stenni, B., Curran, M. A. J., Abram, N. J., Orsi, A., Goursaud, S., Masson-Delmotte, V., Neukom, R., Goosse,  
689 H., Divine, D., van Ommen, T., Steig, E. J., Dixon, D. A., Thomas, E. R., Bertler, N. A. N., Isaksson,  
690 E., Ekaykin, A., Werner, M., and Frezzotti, M.: Antarctic climate variability on regional and  
691 continental scales over the last 2000 years, *Clim. Past*, 13, 1609-1634, 10.5194/cp-13-1609-2017,  
692 2017.

693 Suzuki, K., Yamanouchi, T., Kawamura, K., and Motoyama, H.: The spatial and seasonal distributions of air-  
694 transport origins to the Antarctic based on 5-day backward trajectory analysis, *Polar Science*, 7, 205-  
695 213, <https://doi.org/10.1016/j.polar.2013.08.001>, 2013.

Formatted: Font: (Default) Times New Roman, 10 pt

Formatted: Font: (Default) Times New Roman, 10 pt

Formatted: Font: (Default) Times New Roman, 10 pt

Formatted: Font: (Default) Times New Roman, 10 pt

Formatted: Font: (Default) Times New Roman, 10 pt

Formatted: Font: (Default) Times New Roman, 10 pt

Formatted: Font: (Default) Times New Roman, 10 pt

Formatted: Font: (Default) Times New Roman, 10 pt

Formatted: Font: (Default) Times New Roman, 10 pt

Formatted: Font: (Default) Times New Roman, 10 pt

696 Tetzner, D. R., Thomas, E. R., and Allen, C. S.: Marine diatoms in ice cores from the Antarctic Peninsula and  
697 Ellsworth Land, Antarctica – species diversity and regional variability, *The Cryosphere Discuss.*, 2021,  
698 1–32, 10.5194/tc-2021-160, 2021a.

699 Tetzner, D. R., Thomas, E. R., Allen, C. S., and Piermattei, A.: Evidence of Recent Active Volcanism in the  
700 Balleny Islands (Antarctica) From Ice Core Records, *Journal of Geophysical Research: Atmospheres*,  
701 126, e2021JD035095, <https://doi.org/10.1029/2021JD035095>, 2021b.

702 Thomas, E. R.: Antarctic regional snow accumulation composites over the past 1000 years" v2 , [dataset],  
703 doi:10.5285/cc1d42de-dfe6-40aa-a1a6-d45cb2fc8293, 2017.

704 Thomas, E. R., Marshall, G. J., and McConnell, J. R.: A doubling in snow accumulation in the western Antarctic  
705 Peninsula since 1850, *Geophysical Research Letters*, 35, <https://doi.org/10.1029/2007GL032529>, 2008.

706 Thomas, E. R., Vladimirova, D., and Tetzner, D. R.: CLIVASH2k Antarctic ice core chemistry database  
707 (Version 1.0) [Data set]. [dataset], [https://doi.org/10.5285/9E0ED16E-F2AB-4372-8DF3-  
708 FDE7E388C9A7](https://doi.org/10.5285/9E0ED16E-F2AB-4372-8DF3-FDE7E388C9A7), 2022.

709 Thomas, E. R., Dennis, P. F., Bracegirdle, T. J., and Franzke, C.: Ice core evidence for significant 100-year  
710 regional warming on the Antarctic Peninsula, *Geophysical Research Letters*, 36,  
711 <https://doi.org/10.1029/2009GL040104>, 2009.

712 Thomas, E. R., Allen, C. S., Etourneau, J., King, A. C. F., Severi, M., Winton, V. H. L., Mueller, J., Crosta, X.,  
713 and Peck, V. L.: Antarctic Sea Ice Proxies from Marine and Ice Core Archives Suitable for  
714 Reconstructing Sea Ice over the Past 2000 Years, *Geosciences*, 9, 506, 2019.

715 Thomas, E. R., van Wessem, J. M., Roberts, J., Isaksson, E., Schlosser, E., Fudge, T. J., Vallelonga, P., Medley,  
716 B., Lenaerts, J., Bertler, N., van den Broeke, M. R., Dixon, D. A., Frezzotti, M., Stenni, B., Curran, M.,  
717 and Ekaykin, A. A.: Regional Antarctic snow accumulation over the past 1000 years, *Clim. Past*, 13,  
718 1491–1513, 10.5194/cp-13-1491-2017, 2017.

719 Tierney, J. E., Abram, N. J., Anchukaitis, K. J., Evans, M. N., Giry, C., Kilbourne, K. H., Saenger, C. P., Wu, H.  
720 C., and Zinke, J.: Tropical sea surface temperatures for the past four centuries reconstructed from coral  
721 archives, *Paleoceanography*, 30, 226–252, <https://doi.org/10.1002/2014PA002717>, 2015.

722 Turner, J., Comiso, J. C., Marshall, G. J., Lachlan-Cope, T. A., Bracegirdle, T., Maksym, T., Meredith, M. P.,  
723 Wang, Z., and Orr, A.: Non-annular atmospheric circulation change induced by stratospheric ozone  
724 depletion and its role in the recent increase of Antarctic sea ice extent, *Geophysical Research Letters*,  
725 36, 10.1029/2009gl037524, 2009.

726 Turner, J., Holmes, C., Caton Harrison, T., Phillips, T., Jena, B., Reeves-Francois, T., Fogt, R., Thomas, E. R.,  
727 and Bajish, C. C.: Record Low Antarctic Sea Ice Cover in February 2022, *Geophysical Research  
728 Letters*, 49, e2022GL098904, <https://doi.org/10.1029/2022GL098904>, 2022.

729 Turner, J., Lu, H., White, I., King, J. C., Phillips, T., Hosking, J. S., Bracegirdle, T. J., Marshall, G. J.,  
730 Mulvaney, R., and Deb, P.: Absence of 21st century warming on Antarctic Peninsula consistent with  
731 natural variability, *Nature*, 535, 411–415, 10.1038/nature18645, 2016.

732 WAIS\_Divide\_Project\_Members.: Onset of deglacial warming in West Antarctica driven by local orbital  
733 forcing, *Nature*, 500, 440–444, 10.1038/nature12376, 2013.

734 WAISDivideProjectMembers, Fudge, T. J., Steig, E. J., Markle, B. R., Schoenemann, S. W., Ding, Q., Taylor,  
735 K. C., McConnell, J. R., Brook, E. J., Sowers, T., White, J. W. C., Alley, R. B., Cheng, H., Clow, G.  
736 D., Cole-Dai, J., Conway, H., Cuffey, K. M., Edwards, J. S., Lawrence Edwards, R., Edwards, R.,  
737 Fegyveresi, J. M., Ferris, D., Fitzpatrick, J. J., Johnson, J., Hargreaves, G., Lee, J. E., Maselli, O. J.,  
738 Mason, W., McGwire, K. C., Mitchell, L. E., Mortensen, N., Neff, P., Orsi, A. J., Popp, T. J., Schauer,  
739 A. J., Severinghaus, J. P., Sigl, M., Spencer, M. K., Vaughn, B. H., Voigt, D. E., Waddington, E. D.,  
740 Wang, X., and Wong, G. J.: Onset of deglacial warming in West Antarctica driven by local orbital  
741 forcing, *Nature*, 500, 440–444, 10.1038/nature12376, 2013.

742 Winski, D. A., Osterberg, E. C., Kreutz, K. J., Ferris, D. G., Cole-Dai, J., Thundercloud, Z., Huang, J.,  
743 Alexander, B., Jaeglé, L., Kennedy, J. A., Larrick, C., Kahle, E. C., Steig, E. J., and Jones, T. R.:  
744 Seasonally Resolved Holocene Sea Ice Variability Inferred From South Pole Ice Core Chemistry,  
745 *Geophysical Research Letters*, 48, e2020GL091602, <https://doi.org/10.1029/2020GL091602>, 2021.

746 Wolff, E. W.: Chemical signals of past climate and environment from polar ice cores and firm air, *Chemical  
747 Society Reviews*, 41, 6247–6258, 10.1039/C2CS35227C, 2012.

748 Wolff, E. W., Fischer, H., Fundel, F., Ruth, U., Twarloh, B., Littot, G. C., Mulvaney, R., Rothlisberger, R., de  
749 Angelis, M., Boutron, C. F., Hansson, M., Jonsell, U., Hutterli, M. A., Lambert, F., Kaufmann, P.,  
750 Stauffer, B., Stocker, T. F., Steffensen, J. P., Bigler, M., Siggaard-Andersen, M. L., Udisti, R., Becagli,  
751 S., Castellano, E., Severi, M., Wagenbach, D., Barbante, C., Gabrielli, P., and Gaspari, V.: Southern  
752 Ocean sea-ice extent, productivity and iron flux over the past eight glacial cycles, *Nature*, 440, 491–  
753 496, 2006.

754 Zwally, H. J., Comiso, J. C., Parkinson, C. L., Cavalieri, D. J., and Gloersen, P.: Variability of Antarctic sea ice  
755 1979–1998, *Journal of Geophysical Research: Oceans*, 107, 9-1-9-19, 10.1029/2000jc000733, 2002.

Formatted: Font: (Default) Times New Roman, 10 pt

Formatted: Font: (Default) Times New Roman, 10 pt

Formatted: Font: (Default) Times New Roman, 10 pt

Formatted: Font: (Default) Times New Roman, 10 pt

Formatted: Font: (Default) Times New Roman, 10 pt

Formatted: Font: (Default) Times New Roman, 10 pt

Formatted: Font: (Default) Times New Roman, 10 pt

Formatted: Font: (Default) Times New Roman, 10 pt

Formatted: Font: (Default) Times New Roman, 10 pt

Formatted: Font: (Default) Times New Roman, 10 pt

Formatted: Font: (Default) Times New Roman, 10 pt

Formatted: Font: (Default) Times New Roman, 10 pt

Formatted: Font: (Default) Times New Roman, 10 pt

Formatted: Font: (Default) Times New Roman, 10 pt

|756

**Formatted:** Indent: Left: 3.81 cm, Don't add space between paragraphs of the same style, Line spacing: single